Effect of Base on the Solution Behavior of Oxo(D-penicillaminato)(L-penicillaminato)rhenate(V)

Lory Hansen,[†] Xiaolong Xu,[†] Kwok To Yue,[‡] Andrew Taylor, Jr.,[†] and Luigi G. Marzilli*[,§]

Departments of Radiology, Physics, and Chemistry, Emory University, Atlanta, Georgia 30322

Received November 9, 1995[⊗]

The effect of base on the solution behavior of oxo(D-penicillaminato)(L-penicillaminato)rhenate(V) (**1**) was investigated by ^{1}H NMR, resonance Raman, and UV−visible spectroscopy. The ^{1}H NMR spectrum of **1** consisted of two sets of sharp pen signals in DMSO-d_6 and D_2O below pH 8 (penicillamine = $penH_4$, the subscript on H indicating the number of dissociable protons present). The data were consistent with ReO(D-$penH_3$)(L-$penH_2$) and its enantiomer ReO(L-$penH_3$)(D-$penH_2$), with $penH_3$ coordinated by N, S, and carboxyl O. These enantiomers have a *cis*-N_2,*cis*-S_2 coordination of the pen ligands, both CO_2 groups *anti* to the oxo ligand and one CO_2 coordinated *trans* to the oxo ligand (form **I**). In D_2O, between pH 8.6 and 10.1, the signals broadened, collapsed, and re-emerged as one set of signals, but no accompanying changes were observed in either the resonance Raman or the UV−visible spectra. The NMR spectral changes were attributed to base-catalyzed interconversion between two enantiomers; both CO_2 groups are deprotonated in D_2O, and they alternate between ligated and deligated states. Near pH 11, a new form (**II**) in slow exchange with form **I** was detected by NMR spectroscopy. The Re=O Raman band of **I** (963 cm^{-1}) was replaced by a new midfrequency band (930 cm^{-1}). The UV−visible bands (346 and 492 nm) decreased in intensity. With increasing pH and near pH 12, the ^{1}H NMR signals of **II** shifted. The midfrequency Re=O band was replaced by a low-frequency band (845 cm^{-1}), and both the UV and visible bands continued to decline as new shorter wavelength bands emerged. These spectral changes were consistent with deprotonation of **II** to give **II′**. The ^{1}H NMR spectra of **1** and ReO(D-$penH_3$)(D-$penH_2$) were nearly identical at pH 12. At this pH, the latter complex is a *trans*-dioxo species with a Re=O band at 846 cm^{-1}; the similar NMR spectrum and Re=O band of **1** suggest that **II′** is a *trans*-dioxo species also. This conclusion was supported by studies in methanol which showed that [ReO(OCH_3)(D-$penH_2$)(L-$penH_2$)]$^{2-}$ did not deprotonate.

Introduction

Complexes of the type $M^VO(NS)_2$ and $M^VO(N_2S_2)$ (M = Tc, Re) are common in radiopharmaceutical chemistry because N and S donor atoms stabilize the $[M^VO]^{3+}$ core, which is readily accessible in aqueous solution. Since carboxyl groups are important for recognition by the renal tubular transport system, complexes with ligands derived from cysteine ($cysH_4$, the subscript on H indicating the number of dissociable protons present) (Chart 1) have been investigated as potential renal imaging agents. One such complex, the $^{99m}Tc^VO(N_2S_2)$ complex with *N*,*N*′-ethylenedi-L-cysteine (LL-ECH_6) (Chart 1), shows promise as a renal radiopharmaceutical and is being investigated for clinical use.[1−5]

In our search for the optimal structural requirements for renal tubular transport, we investigated the solution behavior of ReO(LL-ECH_3).[6] The tetramethyl analogs (derived from penicillamine ($penH_4$) (Chart 1)) ReO(DD-$TMECH_3$)[6] and ReO(D-$penH_3$)(D-$penH_2$)[7] were also studied because they provided more useful ^{1}H NMR spectra. (The H_α/Me_β′/Me_β″ spins are not coupled.) Both ReO(LL-ECH_3)[6] and ^{99}TcO(D-$penH_3$)(D-$penH_2$)[8] have a *cis*-N_2,*cis*-S_2 geometry. This N_2S_2 geometry will apply to all compounds discussed in this report unless specified otherwise. Thus, with DD or LL stereochemistry one carboxyl group is *syn* and the other is *anti* to the oxo ligand. In their neutral solid-state forms, the complexes are six-coordinate with the *anti*-CO_2 bound *trans* to the oxo ligand.[6,8] The complexes are potentially triprotic acids; in solution at pH ∼6 the *syn*-CO_2 is deprotonated, while the *anti*-CO_2 remains coordinated (Scheme 1).

Chart 1

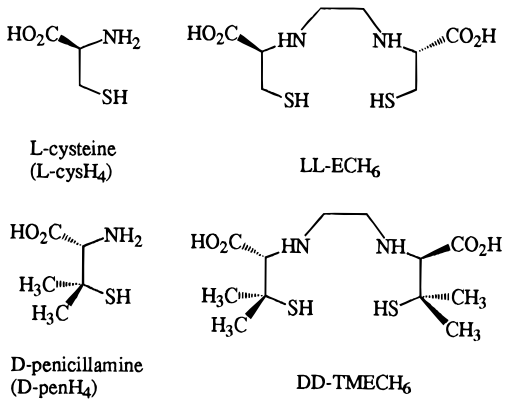

[†] Department of Radiology.
[‡] Department of Physics.
[§] Department of Chemistry.
[⊗] Abstract published in *Advance ACS Abstracts,* April 15, 1996.

(1) Van Nerom, C. G.; Bormans, G. M.; De Roo, M. J.; Verbruggen, A. M. *Eur. J. Nucl. Med.* **1993**, *20*, 738.
(2) Ozker, K.; Onsel, C.; Kabasakal, L.; Sayman, H. B.; Uslu, I.; Bozluolcay, S.; Cansiz, T.; Kapicioglu, T.; Urgancioglu, I. *J. Nucl. Med.* **1994**, *35*, 840.
(3) Stoffel, M.; Jamar, F.; Van Nerom, C.; Verbruggen, A.; Mourad, M.; Leners, N.; Squifflet, J.-P.; Beckers, C. *J. Nucl. Med.* **1994**, *35*, 1951.
(4) Kabasakal, L.; Turoglu, T.; Onsel, C.; Ozker, K.; Uslu, I.; Atay, S.; Cansiz, T.; Sonmezoglu, K.; Altiok, E.; Isitman, A. T.; Kapicioglu, T.; Urgancioglu, I. *J. Nucl. Med.* **1995**, *36*, 224.
(5) Taylor, A., Jr.; Hansen, L.; Eshima, D.; Malveaux, E.; Folks, R.; Shattuck, L.; Lipowska, M.; Marzilli, L. G. *J. Nucl. Med.*, submitted.
(6) Marzilli, L. G.; Banaszczyk, M. G.; Hansen, L.; Kuklenyik, Z.; Cini, R.; Taylor, A., Jr. *Inorg. Chem.* **1994**, *33*, 4850.
(7) Hansen, L.; Xu, X.; Yue, K. T.; Kuklenyik, Z.; Taylor, A., Jr.; Marzilli, L. G. *Inorg. Chem.*, in press.
(8) Franklin, K. J.; Howard-Lock, H. E.; Lock, C. J. L. *Inorg. Chem.* **1982**, *21*, 1941.

S0020-1669(95)01446-7 CCC: $12.00

Scheme 1

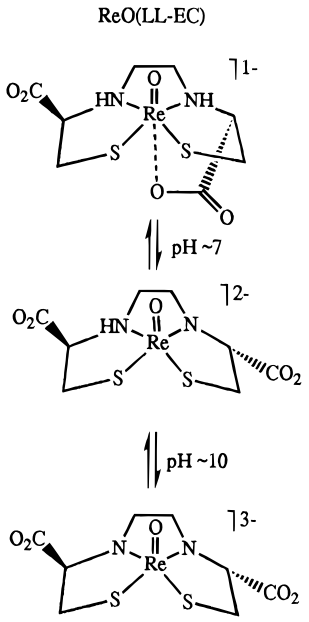

Scheme 2

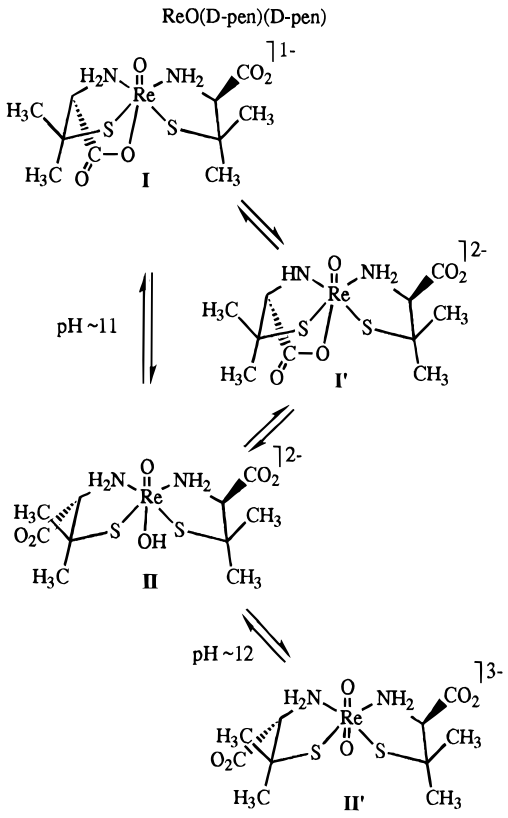

However, NH deprotonation occurs near neutral pH for [ReO(LL-ECH$_2$)]$^-$ and [ReO(DD-TMECH$_2$]$^-$; deprotonation is coupled to CO_2 deligation. The resulting [ReO(LL-ECH)]$^{2-}$ and [ReO(DD-TMECH)]$^{2-}$ anions are most likely five-coordinate.[6] For [ReO(D-penH$_2$)(D-penH$_2$)]$^-$ (form **I**),[7] changes did not occur until a much higher pH value. NH deprotonation and CO_2 deligation occurred independently near pH 11, resulting in an equilibrium mixture of N-deprotonated CO_2-ligated (form **I′**) and N-protonated CO_2-deligated species (Scheme 2). Solvent coordinated to the CO_2-deligated species, and in aqueous solution six-coordinate [ReO(OH)(D-penH$_2$)$_2$]$^{2-}$ (**II**) and [ReO$_2$(D-penH$_2$)$_2$]$^{3-}$ (**II′**) species were formed, each with two trans axial O donor ligands.

An important conclusion from these studies was that the predominant form at physiological pH differs between the EC- and pen-type complexes. These differences between the ReO(N$_2$S$_2$)- and ReO(NS)$_2$-type complexes were attributed to the additional chelate ring in the EC-type complexes. The presence of the ethylene bridge in the EC-type ligand increases the facility of NH deprotonation and also favors deligation of the *anti*-CO_2 group. Such results on the number of species present and the overall charge dictated by the chelate ligand protonation state have provided valuable insights into the future design of radiopharmaceuticals which would exist in only one form.

Since stereochemistry often affects the *in vivo* behavior of small molecules, varying the chirality of the cys/pen residues in MO(NS)$_2$- and MO(N$_2$S$_2$)-type complexes provides additional information about factors that influence radiopharmaceutical biodistribution. Variation of stereochemistry can also be useful in elucidating which forms are present in solution. For MO(NS)$_2$ and MO(N$_2$S$_2$) complexes with mixed DL ligand stereochemistry, two *cis*-N$_2$,*cis*-S$_2$ isomers are possible with both carboxyl groups either *syn* or *anti* to the oxo ligand. In this report we describe the solution behavior of ReO(D-penH$_3$)(L-penH$_2$) (**1**), a representative of the MO(NS)$_2$ family of complexes with mixed D-NS and L-NS ligands.

Experimental Section

UV−visible (UV−vis) titrations were recorded in D_2O on Shimadzu 3101 and Varian Cary 3 instruments; the pH (uncorrected) was adjusted with NaOD (2.2 M) and DCl (2.2 M). High-performance liquid chromatography (HPLC) was carried out on a Beckman Model 332 system equipped with a Model 153 UV detector (254 nm) and automatic integrator. Analytical separations were performed on an Ultrasphere ODS 5 μm 4.6 × 250 mm column utilizing a 12% EtOH, 0.01 M NaH_2PO_4, pH 7.0 mobile phase at a flow rate of 1 mL/min. Elemental analyses were obtained from Atlantic Microlabs, Atlanta, GA.

^{1}H NMR Spectroscopy. Spectra were recorded in D_2O or 75% CD_3OD/D_2O on a Nicolet 360 or a GE 500 NMR spectrometer and processed with FELIX (Hare Research, Inc.) or MacNMR 5.1. Chemical shifts (ppm) were referenced to TSP (3-(trimethylsilyl)-propionic-*2,2,3,3-d*$_4$ acid, sodium salt). The pH (uncorrected) was adjusted with NaOD (2.2 M) or DCl (2.2 M) and NaOD/75% CD_3OD (2.2 M) and measured with a long-stem pH electrode.

Resonance Raman Spectroscopy. Resonance Raman measurements on samples in melting point capillaries were made with excitations at 406.7 nm from a krypton ion laser (Coherent Innova 100). Power at the samples was kept below 20 mW. Raman signals were collected via 90° geometry by a triple monochromator (Spex Model 1877 Triplemate) with a photodiode array detector consisting of a Model IRY-1024 detector and a Model ST-120 controller from Princeton Instruments that was interfaced to an IBM-AT microcomputer. Calibrations were performed for each measurement by using known Raman lines of toluene. Peak positions were accurate to within ±1−2 cm^{-1} between runs. Typical resolution was 6−8 cm^{-1}. For all samples, no changes (both spectral features and intensities) were observed in the Raman spectra as a function of laser exposure time. Concentrations of the Re complexes were ∼40 mM; the pH (uncorrected) was adjusted with NaOD (2.2 M) or DCl (2.2 M) and NaOD/75% CD_3OD (2.2 M).

ReO(D-penH$_3$)(L-penH$_2$) (1). Method A. The procedure described for the preparation of ReO(D-penH$_3$)(D-penH$_2$) (**2**)[7,9] was followed using an excess of DL-penH$_4$ (200 mg, 1.3 mmol) in place of D-penH$_4$. After a 10-min stirring period at room temperature, the reaction solution was neutralized with 1 N NaOH. Aliquots (250 μL) of this solution were subjected to HPLC on an Ultrasphere ODS 5 μm 10 × 250 mm column using a 12% EtOH 0.01 M NaH_2PO_4 pH 7.0 mobile phase at a flow rate of 2 mL/min. The fractions containing **1** were collected, combined, and reduced to a yellow-brown solution (∼1 mL) by rotary evaporation. Phosphate was separated from **1** by passing the solution through a

(9) Johnson, D. L.; Fritzberg, A. R.; Hawkins, B. L.; Kasina, S.; Eshima, D. *Inorg. Chem.* **1984**, *23*, 4204.

Sephadex G-15 column eluted with H_2O. The yellow-brown fraction was collected and the solvent evaporated to near dryness. Green-brown crystals were collected and vacuum-dried. Yield: 15 mg (6%).

Method B. The procedure described in Method A was followed using 2 equiv of DL-penH$_4$ (149 mg, 1.0 mmol). The reaction solution, stirred for 10 min at room temperature, was then left to stand at the same temperature. After 2−3 days, green-brown crystals formed and were collected. Yield: 35 mg (14%). Anal. Calcd for $C_{10}H_{19}N_2O_5ReS_2$: C, 24.14; H, 3.85; N, 5.63. Found: C, 24.30; H, 3.85; N, 5.50.

Results

Synthesis. ReO(D-penH$_3$)(L-penH$_2$) (**1**) was prepared by a literature procedure for ReO(D-penH$_3$)(D-penH$_2$) (**2**).[7,9] This method, Method A, involves an *excess* of ligand. When racemic penH$_4$ was employed, a mixture of DL, DD, and LL products was obtained. Partial solvent reduction by rotary evaporation and cooling the solution to 5 °C afforded only violet DD+LL microcrystals. Johnson et al.[9] previously reported a method for isolation of **1** from the DD and LL isomers by HPLC from which a DL:(DD+LL) product ratio of 1:1 was determined (at 340 nm). Our initial analysis of the reaction solution by HPLC gave a DL:(DD+LL) product ratio of 3:2 (at 254 nm), but when the reaction solution was allowed to stand, the DL:(DD+LL) ratio gradually changed over 2 days. At equilibrium the DL:(DD+LL) ratio was 2:3. (A DL:(DD+LL) equilibrium ratio of 2:3 was also obtained from solutions of **1** and DL-penH$_4$ under similar conditions.) Red-brown plates composed of DL and DD+LL in a ratio of 1:1 (by HPLC and NMR) formed after ∼1 week. Consequently, **1** was initially isolated by HPLC according to the method of Johnson et al.[9] However, when 2 equiv of DL-penH$_4$ was used (Method B), the initial DL:(DD+LL) ratio of 3:2 remained constant. Upon standing, the solution yielded green-brown DL crystals. Subsequent fractions yielded a mixture of green-brown DL crystals and violet DD+LL crystals. Therefore, by altering the reaction stoichiometry and carefully monitoring the crystallization process, we circumvented the tedious HPLC isolation step. Although there is more than one possible isomer for **1** (see below), we observed only one by HPLC.

^{1}H NMR Spectroscopy. If the coordination geometry of **1** is *cis*-N$_2$,*cis*-S$_2$ as found in ^{99}TcO(D-penH$_3$)(D-penH$_2$),[8] three geometric isomers are possible. In two, neither CO_2 is coordinated: one has both CO_2 groups *syn* (*syn*-CO$_2$,*syn*-CO$_2$), and the second has both CO_2 groups *anti* (*anti*-CO$_2$,*anti*-CO$_2$). In these two possible geometric isomers, there is a perpendicular plane of symmetry between the D-pen and L-pen coordination planes. The neutral isolated forms would have only one carboxyl protonated. In the third possible geometric isomer (an enantiomeric pair), coordination of one CO_2^- breaks the symmetry plane (*anti*-CO$_2$,*anti*-CO$_2$-bound). Therefore, the presence of two equal-intensity sets of pen ^{1}H NMR signals for **1** in DMSO-d_6 or D_2O is consistent with either (i) an equal distribution of *syn*-CO$_2$,*syn*-CO$_2$ and *anti*-CO$_2$,*anti*-CO$_2$ geometric isomers or (ii) an *anti*-CO$_2$,*anti*-CO$_2$-bound enantiomeric pair. Since **1** eluted as one peak by HPLC, the latter interpretation (structure **A**) is more likely and agrees with the interpretation proposed by Johnson et al.[9] As mentioned above, there

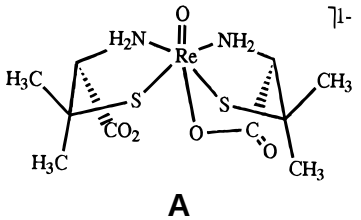

A

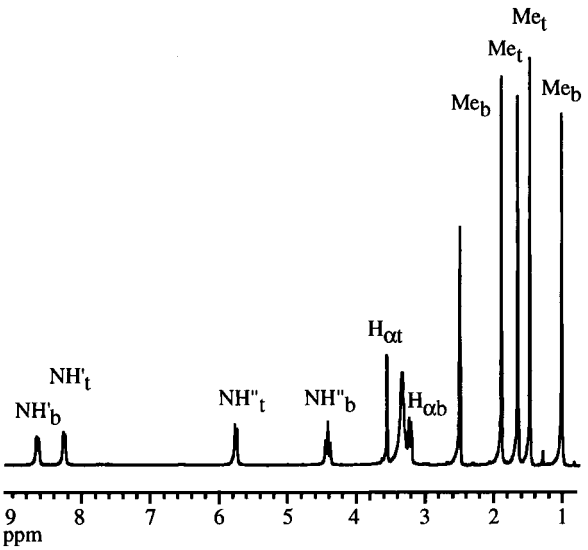

Figure 1. ^{1}H NMR spectrum of ReO(D-penH$_3$)(L-penH$_2$) (**1**) in DMSO-d_6 (b = bidentate, *anti*-CO$_2$; t = tridentate, *anti*-CO$_2$-bound).

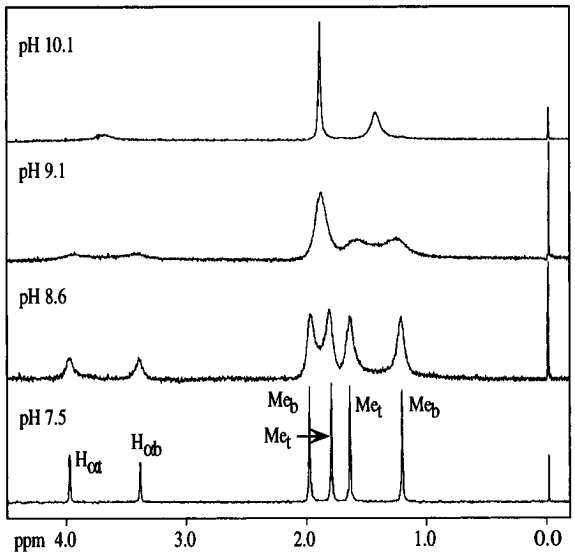

Figure 2. ^{1}H NMR spectrum of ReO(D-penH$_3$)(L-penH$_2$) (**1**) in D_2O at pH values ranging from 7.5 to 10.1 (b = bidentate, *anti*-CO$_2$; t = tridentate, *anti*-CO$_2$-bound).

are no other HPLC peaks attributable to a second DL species, indicating that the *syn*-CO$_2$,*syn*-CO$_2$ species was not formed or, if formed, rapidly converted to the *anti*-CO$_2$,*anti*-CO$_2$-bound form.

The ^{1}H NMR signals of **1** were assigned in DMSO-d_6. The NH and H$_\alpha$ signals were assigned by correlating the magnitude of coupling with the torsion angles between the protons of the *syn*- and *anti*-pen ligands. The Me signals were assigned by comparing their chemical shifts with the those of the Me signals of ReO(D-penH$_3$)(D-penH$_2$) (**2**) (Table 1). In D_2O, the signal assignments for **1** were obtained by following the signals in DMSO-d_6/D_2O mixtures.

In D_2O, the ^{1}H NMR spectrum of **1** changed significantly as the pH was raised from 7.5 (Figure 2). Between pH 8.6 and pH 10.1, the Me′, Me″, and H$_\alpha$ signals of each pen ligand broadened and collapsed into the baseline, and a new single set of Me′, Me″, and H$_\alpha$ signals emerged. At pH 10.1, the chemical shifts of the single set of signals were at the midpoints between the two H$_\alpha$, the two Me′, and the two Me″ signals, respectively, observed at pH 7.5.

At pH 11.1, a second single set of pen signals appeared (Figure 3). With increasing pH, the original single set of signals

Table 1. ^{1}H Chemical Shift Assignments (ppm) for ReO(D-penH$_3$)(L-penH$_2$) (**1**) and ReO(D-penH$_3$)(D-penH$_2$) (**2**)

ReO(D-penH$_3$)(L-penH$_2$) (**1**)

	H_α		Me′/Me″		NH[a]		
solvent	bidentate	tridentate	bidentate	tridentate	bidentate	tridentate	CO_2H
DMSO-d_6	3.24	3.58	1.05, 1.92	1.51, 1.68	8.63′ 4.43″	8.25′ 5.77″	13.77
D_2O, pH 7.5	3.41	4.01	1.22, 2.00	1.66, 1.81			
D_2O, pH 12.4	3.18		1.83	1.15			

ReO(D-penH$_3$)(D-penH$_2$) (**2**)

	Hα		Me′/Me″		NH[a]		
solvent	syn	anti	syn	anti	syn	anti	CO_2H
DMSO-d_6	2.95	3.59	1.27, 1.87	1.44, 1.61	6.57′ 7.58″	5.74′ 7.69″	13.44
D_2O, pH 7.6	3.12	4.07	1.28, 2.07	1.66, 1.83			
D_2O, pH 12.2	3.19		1.83	1.16			

[a] NH′ *syn*, NH″ *anti*.

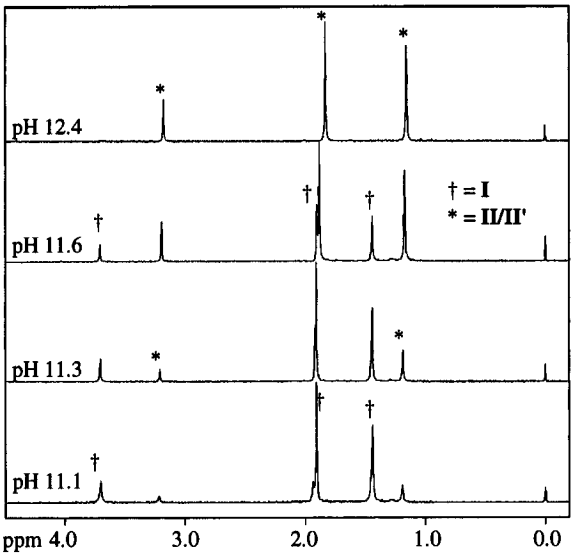

Figure 3. ^{1}H NMR spectrum of ReO(D-penH$_3$)(L-penH$_2$) (**1**) in D_2O at pH values ranging from 11.1 to 12.4.

decreased without any change in chemical shift. Concurrently, the new signals increased in intensity and each signal shifted upfield. At pH 12.4, only the second single set of pen signals was present.

The NMR data suggest that the low-pH form of **1** (**I**) is involved in an exchange process that is slow on the NMR time scale below pH 8. As the pH was raised, the rate of exchange increased and passed through the intermediate and into the fast NMR time domain. Above pH 11, **I** converted to a new high-pH form (**II**). However, **II** converted to a related species (**II′**) as the pH was raised since the high-pH signals shifted with increasing pH. An important observation is that the spectra of **1** and ReO(D-penH$_3$)(D-penH$_2$), **2**, were remarkably similar at pH ∼12. Both complexes had a single set of pen signals, and the chemical shifts of the corresponding signals of **1** (pH 12.4) and **2** (pH 12.2) differed by only ±0.01 ppm.[7] In contrast, at pH 7−8, the signals differed by as much as 0.19 ppm.

In 75% CD_3OD, addition of NaOD produced changes similar to those observed in 100% D_2O. The two sets of pen signals present at neutral pH broadened and re-emerged as one set of signals as the pH was raised. The pH required for these changes was ∼0.5 pH unit higher in 75% CD_3OD than in D_2O. At pH 11.7, new signals began to emerge. As the pH was raised, the original signals declined, and at pH 12.3 and above, a new high-pH form with one set of pen signals (similar to **II**) was the predominant form present; however, the high-pH signals did not shift with increasing pH. Other unidentified but less intense signals were also present at pH 11.7 and above.

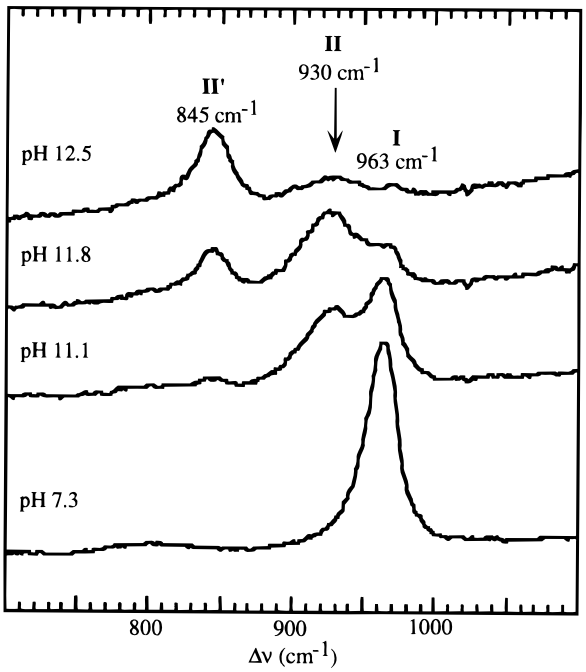

Figure 4. Resonance Raman spectra of ReO(D-penH$_3$)(L-penH$_2$) (**1**) in D_2O at various pH values.

Resonance Raman Spectroscopy. In D_2O, a strong high-frequency Re═O resonance Raman band (963 cm^{-1}) was observed for **1** at pH values ≤10.7. A new, broader midfrequency band (930 cm^{-1}) appeared at pH 11.1 (Figure 4). With increasing pH, the new band increased in intensity while the high-frequency band decreased in intensity. At pH 11.8, a weak low-frequency band (845 cm^{-1}) emerged. As the pH was raised further, the intensity of the low-frequency band increased and that of the midfrequency band decreased. At pH 12.5, the low-frequency band predominated even though the high-frequency and midfrequency bands were still distinguishable.

The changes in the NMR spectrum between pH 8.6 and 10.1 were not accompanied by changes in the Re═O band. However, as the high-pH form observed by NMR (**II**) emerged, so did the midfrequency Re═O band. As the NMR signals at high-pH shifted upfield consistent with a fast **II**/**II′** equilibration, the low-frequency Raman band emerged, identifying it with form **II′**.

In 75% MeOH, the Re═O band at 969 cm^{-1} of form **I** was replaced by a band with a maximum at 916 cm^{-1} between pH

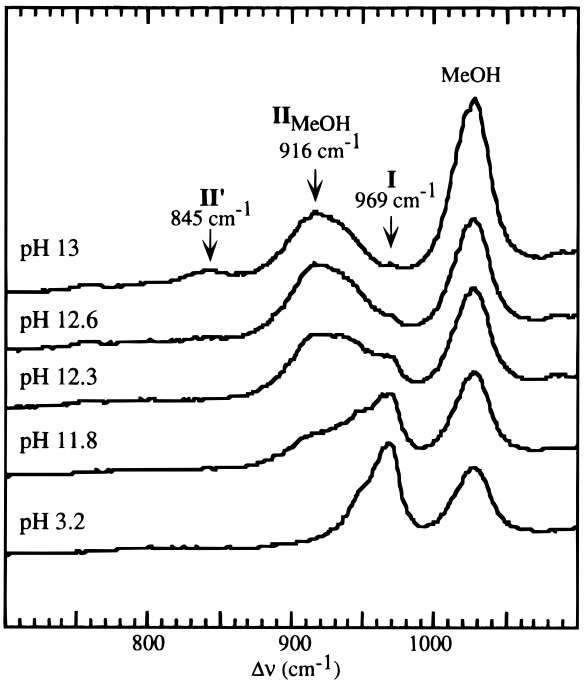

Figure 5. Resonance Raman spectra of ReO(D-penH$_3$)(L-penH$_2$) (**1**) in 75% MeOH at various pH values.

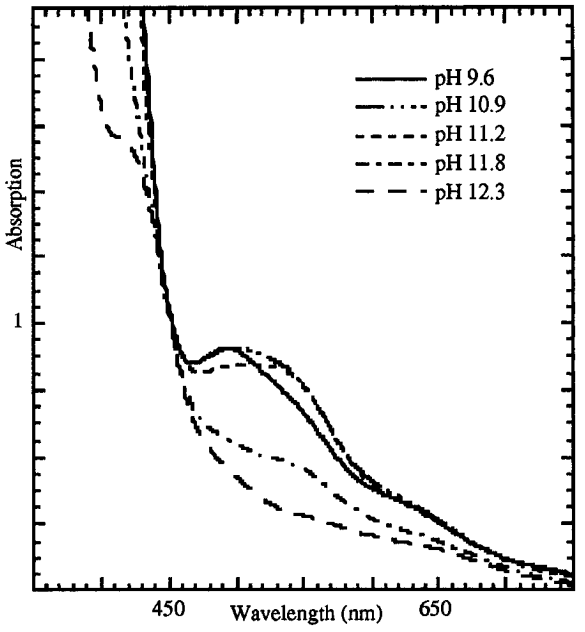

Figure 6. Visible spectra of ReO(D-penH$_3$)(L-penH$_2$) (**1**) (10 mM) in D$_2$O at various pH values (pH 9.6, λ_{max} 493 nm, ϵ 72 M^{-1} cm^{-1}).

11.8 and 12.6 (Figure 5). The new midfrequency band was broad with a high-frequency shoulder. A band at 845 cm^{-1}, characteristic of form **II′**, emerged as the pH approached 13, but it was very much weaker than in 100% D$_2$O.

UV−Visible Spectroscopy. Changes in the UV−vis spectrum of **1** were not observed below pH 10. However, from pH 10.7 to 11.2, the absorption band in the visible region (493 nm) decreased in intensity and developed a shoulder at 550 nm (Figure 6); absorption in the UV region (346 nm) decreased moderately (Figure 7). Above pH 11.2, the intensity of the visible and UV bands decreased sharply and a new UV band at 290 nm emerged. A visible band at 420 nm was not observed until pH 12.3 due to overlap with absorption from the tail of a band in the UV region at lower pH values. The lack of

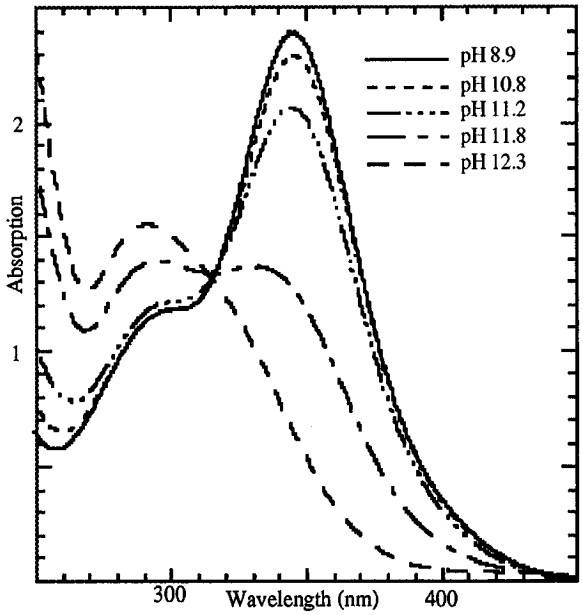

Figure 7. Ultraviolet spectra of ReO(D-penH$_3$)(L-penH$_2$) (**1**) (0.26 mM) in D$_2$O at various pH values (pH 8.9, λ_{max} 346 nm, ϵ 9192 (M^{-1} cm^{-1}); pH 12.3, λ_{max} 290 nm, ϵ 5969 M^{-1} cm^{-1}).

Scheme 3

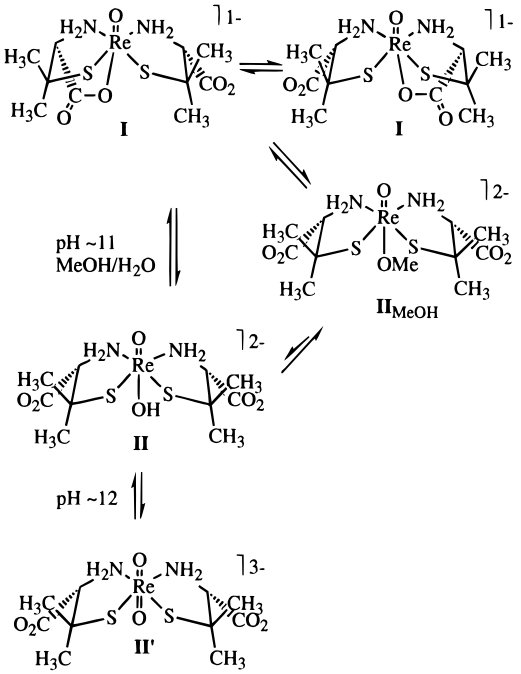

isosbestic points suggests that the low-pH form converted to a pH-dependent mixture of at least two new forms at high-pH.

Discussion

We present our interpretation of the solution results in Scheme 3. A unique feature of ReO(D-penH$_3$)(L-penH$_2$) (**1**) is its ^{1}H NMR spectral behavior from pH 7.5 to 10.1 (Figure 2). The two sets of signals collapsed and re-emerged as one set of sharp signals as the pH was raised. Johnson and co-workers[9] found that as the temperature was increased from 25 to 90 °C at constant neutral pH, all the signals of **1** broadened and collapsed into the baseline and a new, single set of pen signals emerged. These spectral changes were attributed to an increase in the rate of interconversion between two enantiomers of [ReO(D-penH$_2$)-(L-penH$_2$)]$^{-}$ (**I**). The two *anti*-CO$_2$ groups alternate between

ligated and deligated states. Changes in the ^{1}H NMR spectrum of ReO(D-penH$_3$)(D-penH$_2$) (**2**) at elevated temperatures were not observed since, with only one *anti*-CO_2 group, CO_2 exchange is not possible. Our results indicate that increases in hydroxide concentration also increase the rate of interconversion between enantiomers of **1**. No changes were observed in the ^{1}H NMR spectrum of **2** below-pH 10.[7]

Interconversion between enantiomers of [ReO(D-penH$_2$)(L-penH$_2$)]$^-$ (**I**) requires that no new species be formed in this pH range. Both the UV−vis and resonance Raman studies confirm that no new species are formed. Since the OH^- concentration increase did not change the time-averaged NMR shifts of form **I** even above pH 11 (where a second form (**II**) was observed by NMR, Raman, and UV−vis spectroscopy), there was no significant amount of any NH-deprotonated species below pH ~11. The interchange process is simply base-catalyzed. We believe the most likely explanation for this process is that OH^- generates a small (undetectable) amount of an N-deprotonated form. Before rapid reprotonation occurs, the carboxyl group of the deprotonated species deligates with synchronous or nearly synchronous coordination of the carboxyl group of the other pen residue. The four NH groups of form **I** will each be deprotonated by OH^- to some extent. We cannot be sure how many of the four deprotonated forms are kinetically viable intermediates in the exchange process. Since work on ReO(LL-EC) and ReO(DD-TMEC) suggests that deprotonation of the residue with the *anti*-CO_2 bound is favored and leads to deligation,[6] we suspect it may be NH deprotonation of the *anti*-CO_2-bound residue that initiates the exchange between ligated and deligated carboxyl groups.

As the pH was raised further (above 11), a new form (**II**) in slow exchange with the low-pH form (**I**) was evident. **II** gave rise to the midfrequency Raman band and the shoulder (550 nm) in the visible spectrum. We formulate **II** as the OH^--coordinated species (Scheme 3). Although two alternative forms that are NH-deprotonated and either five- or six-coordinate (with H_2O in the axial position) can explain the pH dependence, we rule out these forms on the basis of the following reasoning: First, it is difficult to rationalize how a five-coordinate deprotonated form could be in slow exchange with the low-pH form since the five-coordinate form would have to have a conformation very different from that of the intermediate in the base-catalyzed interconversion of enantiomers of **1**. Furthermore, the activation barrier for forming such a five-coordinate form would have to be larger than the activation barrier between the intermediate and the transition state of the carboxyl deligation−ligation interconversion process. Nevertheless, such a form would have to be more stable than the deprotonated species in the interconversion pathway. It is not clear how such stabilization would occur. Second, if form **II** were an NH-deprotonated species with bound H_2O, the bound water would provide a source of stability. However, water would be weakly bound and it would still be difficult to rationalize why this form would be in slow exchange with form **I**.

Our preferred formulation for **II**, [(ReO(OH)(D-penH$_2$)(L-penH$_2$)]$^{2-}$, accounts for the results better. It could form through an NH-deprotonated intermediate (likely), or it could form directly (less likely). The situation is analogous to the S_N1CB mechanism for base hydrolysis of Co(III) amine acido complexes.[10] The NH undergoes base-catalyzed exchange under conditions in which little or no acido group dissociation has occurred. The NH deprotonation is not detectable directly but is demonstrated by H−D exchange in D_2O at low-pH. In the present case, the NH-deprotonated species is also undetectable, but it leads to the detectable enantiomer interconversion. Since the form of the equilibrium expression for formation of the deprotonated species and the OH^--coordinated species **II** is the same, the value for the equilibrium constant is much higher for forming **II**. **II** must be present but undetectable at low-pH; it becomes detectable only at very high-pH.

Chart 2

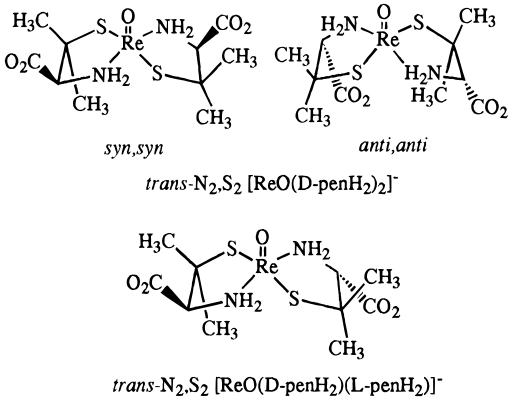

At still higher pH, deprotonation of form **II** occurred. Separate NMR signals were not seen but only upfield shifts of the signals of form **II**. Thus, the high-pH forms (**II** and **II′**) were in fast exchange on the NMR time scale. In the Raman spectrum, the midfrequency and low-frequency bands can be seen. A transition to a higher frequency was observed for the UV band, and the visible band sharply decreased in intensity. These spectroscopic changes can be rationalized as due to either NH or OH deprotonation of form **II** (see below).

It is interesting that the midfrequency Raman species (or mixture of species) was actually more acidic than the low-pH form. The NMR signals for the low-pH form did not shift while those of the high-pH form shifted. This led to the interesting coexistence of Raman bands of all three species! Perhaps electron donation to Re by the oxo group is so diminished (reflected in the lower frequency of the Re═O bond stretch) that OH deprotonation is favored.

The presence of one set of pen signals for forms **II** and **II′** of **1** is readily explained by any of the three possible formulations of **II**. Proton exchange should be rapid in these forms, creating a time-averaged mirror plane. Thus, the rapid interchange between **II** and **II′** cannot necessarily be taken as evidence in favor of axial OH ligation. However, the results do have relevance to our previous work on ReO(D-penH$_3$)(D-penH$_2$) (**2**).

As noted earlier, the ^{1}H NMR spectrum of **2** also has one set of pen signals at pH 12. The apparent symmetry suggested by the NMR spectrum is not so readily explained for **2**, since due to the same configuration of both pen ligands, this complex has one *syn*-CO_2 and one *anti*-CO_2. One hypothesis accounting for the apparent equivalence of the two chelate ligands in **2** is that *cis*-N_2,*cis*-S_2 to *trans*-N_2,*trans*-S_2 isomerization of the bidentate pen ligands has occurred, producing C_2 symmetry about the Re═O axis (Chart 2). This is a reasonable hypothesis since the solid-state structures of a number of five-coordinate $[Re(V)O]^{3+}$ and $[^{99}Tc^{V}O]^{3+}$ complexes with bidentate NS donor ligands have been determined, and the coordination of the NS ligands is often *trans*-N_2,*trans*-S_2.[11−13] If *cis*-N_2,*cis*-S_2 to *trans*-N_2,*trans*-S_2 isomerization occurred for **2**, it would also be

(10) Buckingham, D. A.; Olsen, I. I.; Sargeson, A. M. *J. Am. Chem. Soc.* **1966**, *88*, 5443.

(11) Baldas, J.; Bonnyman, J.; Williams, G. A. *Inorg. Chem.* **1986**, *25*, 150.

(12) Bandolini, G.; Gerber, T. I. A. *Inorg. Chim. Acta* **1987**, *126*, 205.

expected for **1**; however, *cis*-N_2,*cis*-S_2 to *trans*-N_2,*trans*-S_2 isomerization in **1** would destroy *its* symmetry (Chart 2), leading to a doubling of the number of NMR signals. Therefore, the **II** and **II′** forms of **1** cannot be *trans*-N_2,*trans*-S_2. Since the ^{1}H NMR spectra of **1** and **2** at pH ∼12 are strikingly similar and only close inspection reveals that the two spectra are not identical, it is unlikely that basal coordination for **1** is *cis*-N_2,*cis*-S_2 while that for **2** is *trans*-N_2,*trans*-S_2 at high-pH. Thus, we conclude that the *cis*-N_2,*cis*-S_2 → *trans*-N_2,*trans*-S_2 hypothesis is incorrect for both **1** and **2**.

An additional problem with *cis* to *trans* isomerization of **1** is that only one species, a *syn*,*syn* or an *anti*,*anti* species, would be formed stereospecifically (Chart 2). Although such stereoselectivity is possible, the need for it further complicates the hypothesis. This complication adds support to our conclusions that the hypothesis is incorrect.

The apparent symmetry suggested by the ^{1}H NMR spectrum of **2** at high-pH is readily explained by rapid proton exchange, with solvent equilibrating the hydroxo and oxo ligands of $[ReO(OH)(D\text{-penH}_2)_2]^{2-}$. The exchange creates a time-averaged C_2 axis lying in the N_2S_2 plane and bisecting the two ligands. The analogous process for $[ReO(OH)(D\text{-penH}_2)(L\text{-penH}_2)]^{2-}$ leads to a time-averaged mirror plane. The ^{1}H NMR spectra of **1** and **2** are nearly identical at high-pH because the environments of the *syn*- and *anti*-CO_2 groups interchange too fast for differentiation on the NMR time scale.

In contrast to the virtual similarity of the NMR spectra of the **II′** form of **1** and **2** at very high-pH, the pH behavior of the ^{1}H NMR signals of the low-pH form (**I**) of **1** and **2** do differ. The **I** signals of **1** did not shift with increasing pH (Figure 3), but the analogous signals of form **I** of **2** exhibited slight shifts at relatively high-pH (<∼11.7). For **2**, the NMR signals of the low-pH form (**I**) shift, indicating the presence of a fast **I**/**I′** equilibration rate. **I′** is an NH-deprotonated form of **I** (Scheme 2), and **I′** is formed along with **II** in an equilibrium mixture, but the **I′**/**II** equilibration rate is slow.

For **2**, **I′** has an Re═O band (∼930 cm^{-1}) similar in frequency to **II**. Thus, in aqueous solution **I′** and **II** were difficult to distinguish by Raman spectroscopy. In 100% CD_3OD solutions of **2**, the NMR signals of **I** again shifted with addition of base ($NaOCD_3$), indicating that **I′** was formed. The methoxo derivative, $\mathbf{II}_{MeOH}$, was also formed. The Re═O band of $\mathbf{II}_{MeOH}$ is at 916 cm^{-1} and does not overlap severely with the band of **I′** at 933 cm^{-1}. Thus, Raman spectroscopy can distinguish between **I′** (or **II**) and $\mathbf{II}_{MeOH}$.

For **1**, between pH 11.8 and 12.6 in 75% MeOH, the Re═O band for **I** at 969 cm^{-1} decreased and a band at 916 cm^{-1} emerged (Figure 5). A distinct midfrequency band near 930 cm^{-1} was not observed, indicating that neither **I′** nor **II** was formed as a major species in 75% MeOH. The Re═O band of **1** at 916 cm^{-1} was assigned to $\mathbf{II}_{MeOH}$ (Scheme 3) because it was observed only in the presence of MeOH and has a frequency similar to that of a band to assigned to $\mathbf{II}_{MeOH}$ of **2**. The Raman data clearly indicate that formation of $\mathbf{II}_{MeOH}$ is favored over that of **II** in 75% MeOH. Therefore, the NMR signals of **1** that dominated the ^{1}H NMR spectrum in 75% CD_3OD/D_2O above pH 12.3 were assigned to $\mathbf{II}_{MeOD}$.

A slight shoulder at 930 cm^{-1} was evident on the 916 cm^{-1} band of **1** at pH ∼12; this could be due to a small amount of either **I′** or **II**. Near pH 13, the shoulder became weaker and the band characteristic of **II′** appeared. Because the ^{1}H NMR signal of **I** did not shift in 75% CD_3OD, there is no NMR evidence for the formation of the **I′** form of **1**. These sets of results indicate that a small amount of **II** coexists with $\mathbf{II}_{MeOH}$ at pH ∼12 and that **II** is converted to **II′** at pH ∼13. Thus, the Raman results, although complicated, are consistent with the schemes derived from the other spectroscopic measurements.

Differences in the pH behavior of the visible spectra of **1** and **2** in D_2O near pH 11 can also be attributed to the absence and presence of detectable amounts of **I′**, respectively. For **1**, the visible band (Figure 6) decreased in intensity and revealed a shoulder at 550 nm when NMR data showed **I** converted to **II**. Therefore, the weak absorption at ∼550 nm can be attributed to **II**. The **I** and **I′** forms of **2** have similar relatively strong visible bands, and the visible absorption of **II** is probably weak. Thus, little change was observed in the visible spectrum of **2** as **I** converted to **I′** and **II**.

For both **1** and **2**,[7] the Re═O band of $\mathbf{II}_{MeOH}$ was still present, even at extreme pH values (∼13). The ^{1}H NMR signals of $\mathbf{II}_{MeOD}$ did not shift with increasing pH. These results indicate that NH deprotonation of $\mathbf{II}_{MeOH}$ did not occur. Therefore, NH deprotonation of **II** is unlikely to be the process which converts **II** to **II′**. If deprotonation of **II** involves the hydroxo ligand to give a *trans*-dioxo species (**II′**) (Scheme 3), the difference in acidity between **II** and $\mathbf{II}_{MeOH}$ is explained since deprotonation is not possible for the methoxo ligand of $\mathbf{II}_{MeOH}$.

Significant differences also exist between $ReO(D\text{-penH}_3)(L\text{-penH}_2)$ (**1**) and its EC-type analogs ($ReO(DL\text{-ECH}_3)$ and $ReO(DL\text{-TMECH}_3)$. Both *syn* and *anti* isomers of the EC-type complexes are known.[14,15] The *anti* isomers underwent base-catalyzed interconversion between enantiomers below physiological pH; at higher pH values, NH deprotonation was coupled to CO_2 deligation, a process similar to that observed for $ReO(DD\text{-TMECH}_3)$.[6,15] Furthermore, *anti*-$ReO(DL\text{-ECH}_3)$ and *anti*-$ReO(DL\text{-TMECH}_3)$ converted to the *syn* isomers at high-pH (>10) and did not re-form when the pH was lowered.[14] Thus, for the EC-type complexes the *syn* isomer is favored. Although *syn*-$ReO(D\text{-penH}_3)(L\text{-penH}_2)$ would be readily accessible through the high-pH forms (**II**/**II′**) (Scheme 3), only *anti*-$ReO(D\text{-penH}_3)(L\text{-penH}_2)$ was formed.

Conclusions

$ReO(D\text{-penH}_3)(L\text{-penH}_2)$ (**1**) exhibits unique solution behavior due to its mixed DL ligand stereochemistry. Unlike $ReO(D\text{-penH}_3)(D\text{-penH}_2)$,[7] the title complex (**1**) exists as a pair of enantiomers that undergo base-catalyzed interconversion, does not form a CO_2-ligated N-deprotonated species (**I′**) in aqueous solution, and prefers methoxo ligation ($\mathbf{II}_{MeOH}$) over hydroxo ligation (**II**) in its CO_2-deligated form in a methanol/water mixture. Although axial hydroxo coordination is more favored than NH deprotonation in $ReO(D\text{-penH}_3)(L\text{-penH}_2)$ (**1**) compared to $ReO(D\text{-penH}_3)(D\text{-penH}_2)$ (**2**), both add axial hydroxo and are much less prone to NH deprotonation than the EC-type complexes. Thus, the similarities in structure and bonding of the neutral forms of the complexes in the solid state disappear in solution and diverse chemistries become evident, even under physiological conditions.

Acknowledgment. This work was supported by the National Institutes of Health (Grant No. DK38842). We thank the NIH and NSF for supporting the purchase of instruments.

IC951446X

(13) Chi, D. Y.; Katzenellenbogen, J. A. *J. Am. Chem. Soc.* **1993**, *115*, 7405.

(14) Hansen, L.; Lipowska, M.; Taylor, A., Jr.; Marzilli, L. G. *Inorg. Chem.* **1995**, *34*, 3579.

(15) Hansen, L.; Yue, K. T.; Xu, X.; Lipowska, M.; Taylor, A., Jr.; Marzilli, L. G. Manuscript in preparation.